

A Two-Branch Finite-Field Construction for Regular CSS LDPC Bases

Koki Okada and Kenta Kasai
Institute of Science Tokyo
okada.k.3154@m.isct.ac.jp
kenta@ict.eng.isct.ac.jp

Abstract

This paper develops a two-branch multiplicative-coset construction for regular Calderbank–Shor–Steane (CSS) quantum low-density parity-check base matrices. For a target column weight J and an even row weight L , the method reduces regularity, CSS orthogonality, and same-type 4-cycle exclusion to explicit quotient-coset conditions over a finite field. A normalized exhaustive search for these conditions produces base matrices for several (J, L) pairs, so the construction is not tied to a single degree distribution. The construction separates the finite-length design into two stages: the base matrix fixes the degree distribution and the first girth constraints, and a cyclic lift randomizes edge connections subject to exact algebraic checks. As a detailed example, we carry one $(3, 10)$ -regular base through the lift and decoding stages. For this example, the selected 64-fold lift gives a code whose same-type Tanner graphs have girth at least eight, and it also excludes a specified weight-16 nondegenerate logical-support orbit. The resulting instance is a $[[10240, 4108, 10 \leq d \leq 32]]$ CSS code. For decoding, we use joint log-domain belief propagation together with low-complexity deterministic post-processing rules for small residual syndromes, including repairs for residual patterns with two unsatisfied checks. The frame error rate (FER) measurements provide finite-length decoding data for this detailed example; at depolarizing probability $p = 0.058$, the post-processing FER is 1.0×10^{-7} .

1 Introduction

Low-density parity-check (LDPC) codes were introduced as sparse parity-check codes for classical error correction [1]. Their Tanner graphs support iterative message-passing decoders, and this sparse-graph viewpoint became one of the standard foundations of modern coding theory. Classical finite-length LDPC design can be viewed as the simultaneous control of three quantities: degree distribution, girth, and randomness in the edge connections. For a fixed channel and update rule, the variable-node and check-node degree distributions determine the belief-propagation (BP) threshold predicted by density evolution [2]. This made degree-distribution design a central part of LDPC code design, especially for irregular ensembles approaching capacity [3]. At the same time, finite-length decoding is sensitive to short cycles, so the girth and the number of short cycles are also structural design targets. Finally, a favorable degree distribution and a large local girth are not enough if the finite graph still contains deterministic short-cycle or low-weight structures that degrade decoding. The classical ensemble argument therefore relies on randomness in the edge connections: random edge connections, or equivalently random lifts of a base graph, reduce deterministic finite-length structures and make the finite graph locally resemble the ensemble used in BP threshold analysis [4]. The same requirement appears in recent quantum LDPC construction work: after the degree distribution and orthogonality constraints are fixed, additional randomization or randomized local modification is used to avoid deterministic finite-length structures while preserving the sparse CSS constraints [5]. Quantum error correction introduced stabilizer codes and, within them, Calderbank–Shor–Steane (CSS) codes [6, 7]. In the CSS setting, one does not choose

a single sparse parity-check matrix. Instead, one chooses two sparse binary check matrices whose row spaces must satisfy a commutation condition. Recent finite-length quantum LDPC work has studied this constraint from several complementary directions, including non-binary extensions, permutation-based high-girth constructions, degeneracy-aware decoding, and CSS constructions with performance close to coding-theoretic or density-evolution reference points [8, 9, 10, 11].

Quantum LDPC codes inherit the sparse-graph motivation of classical LDPC coding, but they also inherit this additional commutation requirement. Early sparse-graph constructions and iterative decoders established the basic finite-length setting [12, 13]. At the same time, explicit algebraic constructions already showed that commutation is difficult to reconcile with the graph properties that are desirable for iterative decoding, such as regularity and the absence of short cycles [14, 15]. This issue has continued in more recent quasi-cyclic, affine-permutation, and non-binary CSS constructions, where the support structure, field labels, and permutation choices are designed so that orthogonality and short-cycle constraints remain compatible [16, 17, 18]. This commutation constraint remains a central design restriction. Thus, even before optimizing a finite-length decoder implementation, one has to decide which degree distribution to realize and then construct a sparse CSS matrix pair that realizes it without violating commutation. In the present design, randomness is introduced in two controlled stages. At the base-matrix stage, the finite-field construction gives many coefficient choices, and the search selects a base that has the target degrees, CSS orthogonality, and no same-type 4-cycles. At the lift stage, cyclic lift labels are sampled and then checked so that the remaining base 6-cycles do not close and the specified low-weight support pattern is excluded. This separates the roles of the two stages: the base fixes the degree distribution and the first girth constraints, while the lift supplies randomized edge connections subject to exact algebraic checks.

One major line of work addressed asymptotic parameters. Hypergraph-product codes gave a systematic positive-rate construction with square-root distance scaling [19]. Subsequent product and lifted constructions improved the asymptotic picture, first by exceeding square-root distance scaling and then by producing asymptotically good quantum LDPC codes [20, 21, 22]. Recent fixed-degree random CSS constructions also connect the sparse quantum LDPC setting with Gilbert–Varshamov-type distance guarantees [23]. These developments established that sparse quantum codes can simultaneously achieve strong asymptotic rate and distance guarantees.

Another line of work remained focused on finite block lengths, where the main questions are different. At finite length, one must specify an actual sparse matrix pair, verify the commutation condition, control short cycles in the Tanner graphs, identify low-weight logical operators or certified candidates, and evaluate a concrete decoder. In this regime, decoder behavior depends on the interaction between graph structure, degeneracy, and post-processing rules [24, 25]. For that reason, finite-length construction work often proceeds by combining algebraic design, explicit certification, and numerical decoding experiments.

The present paper belongs to this finite-length line. Recent work around this finite-length program separates several tasks that are often combined in direct sparse CSS design: constructing a regular commuting base, adding randomness without destroying orthogonality, certifying short-cycle and low-weight structures, and evaluating belief-propagation-based decoding on a concrete lifted code [5, 11, 26, 27, 28, 29]. The decoding side of the same program includes empirical studies of sharp finite-length transitions and residual error-floor events under joint BP decoding [30]. These cited finite-length constructions provide the immediate context for the present paper, but the specific design used here is different from the previously studied non-binary, affine-permutation, affine-coset, and square-base hypergraph-product constructions.

The detailed example targets a CSS code with column weight three and row weight ten. This degree pair has different constraints from the previously studied cases with the same column weight and row weights eight and twelve. Compared with row weight eight, row weight ten requires more incidences in each check while still controlling same-type short cycles. Compared with row weight

twelve, row weight ten leaves less freedom for arranging the paired cross-type overlaps that enforce CSS orthogonality. The search for this case led to a more general finite-field construction of regular CSS bases. Thus the main design problem in this paper is not only to realize one base with column weight three and row weight ten, but to give a verifiable base-construction principle for many choices of column and row weights.

Our solution is a two-branch multiplicative-coset construction over a finite field. The construction is stated in a field-independent form first, so that the reason for regularity and the sufficient coset conditions used to certify orthogonality and same-type 4-cycle exclusion are explicit. The resulting quotient-coset conditions can be checked by a finite normalized search, and the paper records coefficient examples for several regularities. Among these bases, we select the instance with column weight three and row weight ten as the detailed example and carry it through the finite-length stages: specialization to the field with sixteen elements, selection of a 64-fold cyclic lift, exclusion of the remaining same-type base 6-cycles, and exclusion of a specified weight-16 logical-support orbit. The decoding section then studies this concrete lifted code under joint BP and deterministic post-processing, using the factor-graph formulation in [29].

The position of this paper in the historical development is therefore specific. It does not propose a new asymptotic family, and it does not claim an exact distance theorem for a broad class of codes. Instead, it gives a general finite-field base construction, shows that the construction produces many regular CSS bases, and then treats the base with column weight three and row weight ten as the detailed finite-length example. Choosing lifts, certifying distance, and measuring finite-length decoding performance for the other regularities are left as future work.

2 General Theory of the Two-Branch Finite-Field Base

This section gives the field-independent part of the construction. The purpose is to define the two-branch finite-field incidence rule and to record the general certificates used later. The main outputs of the section are (J, L) regularity, a sufficient coset condition for CSS orthogonality, and a separate sufficient coset condition for excluding same-type 4-cycles.

2.1 Base Incidence Rule

The first construction stage builds the base matrices H_X and H_Z . This is the part of the design where the incidence pattern is chosen explicitly. Before specializing to a concrete field, we record the general incidence rule that specifies the rows, columns, and nonzero positions of the two base matrices. The construction uses translations of a multiplicative subgroup in a finite field to place the ones in H_X and H_Z . Two branches are used because CSS orthogonality is enforced by pairing the X - Z overlaps of branch 0 and branch 1, while same-type 4-cycles are avoided by requiring the corresponding same-type difference cosets to be disjoint. The column weight is denoted by J , and the row weight is denoted by L . The row weight is controlled by the subgroup size: each branch contributes one incident column for each element of M , so the two-branch construction gives

$$L = 2|M|.$$

Thus, to target an even row weight L , one seeks a finite field whose multiplicative group contains a subgroup of order $L/2$.

Definition 1 (Two-branch multiplicative-coset base). Let \mathbb{F} be a finite field and let M be a multiplicative subgroup of \mathbb{F}^\times . Fix a branch index $\lambda \in \{0, 1\}$ and a column weight J . For each branch, choose coefficients

$$a_0^{(\lambda)}, \dots, a_{J-1}^{(\lambda)} \in \mathbb{F}, \quad b_0^{(\lambda)}, \dots, b_{J-1}^{(\lambda)} \in \mathbb{F}.$$

The columns are indexed by

$$(\lambda, t, h) \in \{0, 1\} \times \mathbb{F} \times M.$$

We call λ the branch index, t the translation coordinate, and h the subgroup coordinate of the base column. The X rows and Z rows are indexed by

$$(i, r), \quad i = 0, \dots, J-1, \quad r \in \mathbb{F},$$

and

$$(j, s), \quad j = 0, \dots, J-1, \quad s \in \mathbb{F},$$

respectively. Here i and j are row-group indices, while r and s are field-position coordinates. Define binary matrices H_X and H_Z with these row and column index sets as follows. For brevity, put

$$m_0 = m_X = m_Z = J|\mathbb{F}|.$$

Both matrices have m_0 rows and

$$2|\mathbb{F}||M|$$

columns. When the matrices are displayed or stored as ordinary arrays, fix enumerations

$$\mathbb{F} = \{\alpha_0, \dots, \alpha_{q-1}\}, \quad M = \{\mu_0, \dots, \mu_{m-1}\},$$

where $q = |\mathbb{F}|$ and $m = |M|$, and order the branch indices as 0, 1. The zero-based global row and column coordinates are then

$$\rho_X(i, \alpha_u) = iq + u, \quad \rho_Z(j, \alpha_u) = jq + u, \quad (1)$$

and

$$\kappa(\lambda, \alpha_u, \mu_v) = \lambda qm + um + v. \quad (2)$$

For one-based printed row or column numbers, add 1 to these coordinates. In H_X , column (λ, t, h) has ones in the rows

$$(i, t + a_i^{(\lambda)}h) \quad (i = 0, \dots, J-1) \quad (3)$$

and zeros elsewhere. In H_Z , column (λ, t, h) has ones in the rows

$$(j, t + b_j^{(\lambda)}h) \quad (j = 0, \dots, J-1) \quad (4)$$

and zeros elsewhere. Equivalently, these equations specify the X -side and Z -side incidences of the base Tanner graphs. \square

The next example is included only to make the indexing convention concrete. It is not used as a later code instance; it shows how the abstract row, column, and subgroup coordinates become ordinary binary matrices.

Example 1 (Small $J = 3$ two-branch base). The following small certified instance has $J = 3$, matching the column weight used in the detailed (3, 10) example. Take

$$\mathbb{F} = \mathbb{F}_7, \quad M = \{1, 2, 4\} \subset \mathbb{F}_7^\times, \quad J = 3.$$

Set

$$\mathbf{a}^{(0)} = (0, 1, 3), \quad \mathbf{b}^{(0)} = (2, 4, 5), \quad \mathbf{a}^{(1)} = (0, 3, 1), \quad \mathbf{b}^{(1)} = (4, 2, 5),$$

with entries interpreted modulo 7. Then $m_0 = 21$, the base length is 42, and the row weight is $L = 2|M| = 6$. These coefficients satisfy the coset certificates in Theorems 2 and 3. For example, consider the column indexed by $(\lambda, t, h) = (0, 0, 1)$. Using the incidence rule in Definition 1, this column has ones in H_X at

$$(0, 0 + 0 \cdot 1), \quad (1, 0 + 1 \cdot 1), \quad (2, 0 + 3 \cdot 1),$$

namely at the rows $(0, 0), (1, 1), (2, 3)$. In the displayed H_X^{ex} matrix below, this is the first column, and the corresponding entries are highlighted. The same column has ones in H_Z at

$$(0, 0 + 2 \cdot 1), \quad (1, 0 + 4 \cdot 1), \quad (2, 0 + 5 \cdot 1),$$

namely at the rows $(0, 2), (1, 4), (2, 5)$. In the displayed H_Z^{ex} matrix, the corresponding entries in the same first column are highlighted. For the displayed arrays, use the enumerations $\alpha_u = u$ for \mathbb{F}_7 and $(\mu_0, \mu_1, \mu_2) = (1, 2, 4)$ for M . With the global coordinates in (1) and (2), the resulting binary matrices are

$$H_X^{\text{ex}} = \begin{bmatrix} \text{Matrix 1} \\ \text{Matrix 2} \\ \text{Matrix 3} \end{bmatrix}, \quad H_Z^{\text{ex}} = \begin{bmatrix} \text{Matrix 4} \\ \text{Matrix 5} \\ \text{Matrix 6} \end{bmatrix}$$

The colored backgrounds of the one entries indicate row groups, the yellow entries mark the column used in the preceding calculation, the thick vertical separator marks the branch boundary, the thin vertical separators mark the M -blocks, and the horizontal separator marks the row-group boundary. The unit quantities represented by these separators are as follows: each row has weight $2|M|$, and one branch block contains $J|\mathbb{F}||M|$ one entries. In this example, these numbers are 6 and 63, respectively. \square

2.2 Regularity and Coset Certificates

This definition separates the combinatorial part of the construction from the choice of a particular field. The field and subgroup determine the block length and row weight. The next theorem records the first consequence of this construction rule: the desired regularity is automatic once the index sets have been fixed in this way.

Theorem 1 ((J, L) Regularity). Let H_X and H_Z be the binary matrices of Definition 1. Then (H_X, H_Z) is (J, L) -regular with $L = 2|M|$: every column of H_X and H_Z has weight J , and every row of H_X and H_Z has weight L . \square

Proof. By Definition 1, each column is connected to exactly one row in each of the J row groups on the X side and exactly one row in each of the J row groups on the Z side. Hence every column of H_X and H_Z has weight J . For a fixed X row (i, r) , each pair (λ, h) determines a unique value

$$t = r - a_i^{(\lambda)}h,$$

and hence a unique incident column. Indeed, $a_i^{(\lambda)}h$ is a fixed element of \mathbb{F} , so subtraction in the field gives a single element $t \in \mathbb{F}$. Equivalently, if t and t' both satisfy $r = t + a_i^{(\lambda)}h = t' + a_i^{(\lambda)}h$, then $t = t'$. Thus each X row has weight $L = 2|M|$. The same argument applies to Z rows. This proves the claim. \square

The remaining structural properties depend on the coefficient arrays. The next two theorems separate the two finite-field certificates used in this paper. The first theorem certifies CSS orthogonality from cross-type coset equalities. The second theorem certifies the absence of same-type 4-cycles from same-type coset disjointness. These hypotheses are sufficient for the construction in this paper; they are not claimed to be necessary for every possible two-branch base.

Theorem 2 (CSS Orthogonality). Let H_X and H_Z be the binary matrices of Definition 1. Assume that

$$b_j^{(\lambda)} - a_i^{(\lambda)} \neq 0 \tag{5}$$

for all $\lambda \in \{0, 1\}$ and all i, j . Assume also that

$$(b_j^{(0)} - a_i^{(0)})M = (b_j^{(1)} - a_i^{(1)})M \quad \text{for all } i, j. \tag{6}$$

Then $H_X H_Z^T = 0$ over \mathbb{F}_2 . \square

Proof. By the incidence equations (3) and (4) in Definition 1, an X row (i, r) and a Z row (j, s) share a branch λ column (λ, t, h) exactly when

$$r = t + a_i^{(\lambda)}h, \quad s = t + b_j^{(\lambda)}h.$$

Eliminating t gives

$$s - r = (b_j^{(\lambda)} - a_i^{(\lambda)})h$$

for some $h \in M$. Conversely, if this equation holds for some $h \in M$, then setting $t = r - a_i^{(\lambda)}h$ gives a common column satisfying both (3) and (4). For this fixed h , the value of t is unique by the same field calculation: any t' with $r = t' + a_i^{(\lambda)}h$ must equal $r - a_i^{(\lambda)}h = t$. The nonzero-difference condition (5) makes such an h unique when it exists. Hence the coset equality (6) is a sufficient condition making the branch 0 and branch 1 overlaps identical as subsets of possible differences $s - r$. Every X - Z row overlap is therefore either absent in both branches or present once in each branch, so the binary inner product is even. \square

The next theorem applies the same coset viewpoint to row pairs of the same type. Its role is to guarantee that two X -rows, or two Z -rows, never share two columns.

Theorem 3 (Sufficient Coset Criterion for Same-Type 4-Cycle Exclusion). Let H_X and H_Z be the binary matrices of Definition 1. Assume that

$$a_{i'}^{(\lambda)} - a_i^{(\lambda)} \neq 0, \quad b_{j'}^{(\lambda)} - b_j^{(\lambda)} \neq 0 \tag{7}$$

for all $\lambda \in \{0, 1\}$, all $i < i'$, and all $j < j'$. If, in addition,

$$(a_{i'}^{(0)} - a_i^{(0)})M \cap (a_{i'}^{(1)} - a_i^{(1)})M = \emptyset \quad \text{for all } i < i', \tag{8}$$

and

$$(b_{j'}^{(0)} - b_j^{(0)})M \cap (b_{j'}^{(1)} - b_j^{(1)})M = \emptyset \quad \text{for all } j < j'. \tag{9}$$

Then the Tanner graphs of H_X and H_Z have no same-type 4-cycles. \square

Proof. By the X -side incidence equation (3), two distinct X rows (i, r) and (i', r') share a branch λ column (λ, t, h) exactly when

$$r = t + a_i^{(\lambda)}h, \quad r' = t + a_{i'}^{(\lambda)}h.$$

Eliminating t , this is equivalent to

$$r' - r = (a_{i'}^{(\lambda)} - a_i^{(\lambda)})h.$$

If $i = i'$, then distinctness of the two rows gives $r \neq r'$, so the displayed equation has no solution. Thus same-group row pairs share no column. It remains to consider $i \neq i'$; after relabeling, assume $i < i'$. The nonzero-difference condition (7) then makes h unique when it exists, so a fixed branch contributes at most one common column. Across the two branches, the disjointness condition (8) prevents this row pair from sharing one column in each branch. Thus no X -side row pair shares two columns. The Z -side argument is identical using the disjointness condition (9). \square

2.3 Finite Search and Coefficient Examples

The preceding two theorems reduce the coefficient choice to a finite quotient-coset feasibility problem. The next proposition records this feasibility condition explicitly. It is a necessary and sufficient condition for the coefficients to satisfy the two sufficient certificates used in this construction.

Proposition 1 (Coefficient Feasibility for the Coset Certificates). Let $q = |\mathbb{F}|$, $m = |M|$, and let

$$\pi : \mathbb{F}^\times \rightarrow \mathbb{F}^\times / M$$

be the quotient map. For the two-branch construction to have row weight L through this certificate, one must have $L = 2m$. Thus L is even and $m \mid (q - 1)$. The nonzero-difference assumptions also imply that, in each branch, the $2J$ elements

$$a_0^{(\lambda)}, \dots, a_{J-1}^{(\lambda)}, b_0^{(\lambda)}, \dots, b_{J-1}^{(\lambda)}$$

are distinct, so $q \geq 2J$ is necessary. If $J \geq 2$, the same-type disjointness condition further requires at least two nonzero M -cosets, equivalently $(q - 1)/m \geq 2$.

For a fixed pair (\mathbb{F}, M) , a choice of coefficients satisfies the hypotheses of Theorems 2 and 3 if and only if all differences appearing below are nonzero and

$$\pi(b_j^{(0)} - a_i^{(0)}) = \pi(b_j^{(1)} - a_i^{(1)}) \quad \text{for all } i, j,$$

while

$$\pi(a_{i'}^{(0)} - a_i^{(0)}) \neq \pi(a_{i'}^{(1)} - a_i^{(1)}) \quad \text{for all } i < i',$$

and

$$\pi(b_{j'}^{(0)} - b_j^{(0)}) \neq \pi(b_{j'}^{(1)} - b_j^{(1)}) \quad \text{for all } j < j'.$$

\square

Proof. The identity $L = 2m$ follows from Theorem 1. A subgroup $M \leq \mathbb{F}^\times$ of order m can exist only when $m \mid (q - 1)$. The nonzero-difference conditions (5) and (7) say, in particular, that no two elements among the $a_i^{(\lambda)}$'s and $b_j^{(\lambda)}$'s in the same branch coincide. This gives $q \geq 2J$. When $J \geq 2$, the same-type condition requires two nonzero differences to lie in disjoint nonzero cosets, so at least two nonzero M -cosets are necessary.

For the exact quotient condition, recall that two nonzero elements $x, y \in \mathbb{F}^\times$ generate the same M -coset precisely when $\pi(x) = \pi(y)$. Therefore the cross-type coset equality (6) is exactly the displayed equality for $\pi(b_j^{(\lambda)} - a_i^{(\lambda)})$. Similarly, the same-type coset disjointness conditions (8) and (9) are exactly the displayed inequalities for the corresponding a - and b -differences. Together with the stated nonzero-difference requirement, this is equivalent to satisfying the two coset certificates. \square

Proposition 1 is a finite feasibility test, not an automatic existence theorem for every (J, L) . Nevertheless, the same quotient-coset certificate is not specific to the $(3, 10)$ instance. We used the following normalized exhaustive search. Adding a field element to all $a_i^{(\lambda)}$ and $b_j^{(\lambda)}$ within one branch preserves all differences in that branch, and multiplying all coefficients in both branches by one nonzero field element preserves all quotient-coset equalities and disjointness tests. Thus, without loss of generality for this search, we set

$$a_0^{(0)} = a_0^{(1)} = 0, \quad a_1^{(0)} = 1.$$

After $\mathbf{a}^{(0)}$ and $\mathbf{b}^{(0)}$ in branch 0, and $\mathbf{a}^{(1)}$ in branch 1, are fixed, the orthogonality coset equations restrict each $b_j^{(1)}$ to the finite intersection

$$\bigcap_{i=0}^{J-1} (a_i^{(1)} + (b_j^{(0)} - a_i^{(0)})M).$$

We then test the remaining same-type disjointness conditions. For fixed (\mathbb{F}, M) , this gives a deterministic search of order

$$O\left((q-2)_{2J-2}(q-1)_{J-1}J^2|M|\right),$$

where $(u)_v = u(u-1)\cdots(u-v+1)$. If a coefficient choice satisfying the quotient-coset certificates exists, this normalized exhaustive search finds one up to the stated translation and scaling symmetries. This completeness statement is only for the sufficient certificates in Proposition 1; it does not rule out other CSS bases certified by different arguments.

The use of a finite field is a convenient sufficient framework rather than a logically minimal requirement of the incidence argument. The regularity proof uses only additive translations, while the orthogonality and 4-cycle proofs use the fact that multiplication by each nonzero coefficient difference acts injectively on the subgroup coordinate $h \in M$. Equivalently, the relevant difference orbits must have trivial stabilizer under the action replacing multiplication by M . Thus the same proof strategy should extend to finite additive groups equipped with a semiregular automorphism group, or to finite rings and modules after restricting to coefficient differences for which the chosen unit action is injective. In such a generalization, the quotient-coset tests in Proposition 1 would be replaced by orbit-equality and orbit-disjointness tests. We leave this group-action version of the construction for future work; the present paper stays with finite fields because they make the certificates and the normalized exhaustive search explicit and reproducible.

Table 1 lists coefficient examples found by this search over small finite fields. For the \mathbb{F}_9 row we write $\mathbb{F}_9 = \mathbb{F}_3[\alpha]/(\alpha^2 + 1)$; in the prime-field rows, the entries are integers modulo q . Since the multiplicative group \mathbb{F}^\times of a finite field is cyclic, the subgroup $M \leq \mathbb{F}^\times$ is uniquely determined by the field \mathbb{F} and its order $|M| = L/2$. For this reason, the table does not list the elements of M . The parameter column gives the actual base CSS parameters computed from binary ranks: $n = 2q|M|$ and $k = n - \text{rank}_{\mathbb{F}_2}(H_X) - \text{rank}_{\mathbb{F}_2}(H_Z)$. It also gives the verified information on the base CSS distance $d = \min(d_X, d_Z)$. If the lower and upper bounds agree, the entry is written as $[[n, k, d]]$. If a useful small upper-bound witness is available, the entry is written as $[[n, k, d_L \leq d \leq d_U]]$; if only the certified lower bound is reported, it is written as $[[n, k, d \geq d_L]]$. Lower bounds come from exhaustive exclusion of lower-weight nontrivial logical representatives. Displayed upper bounds come from explicit logical representatives; large upper-bound witnesses are omitted from the table because they give little finite-length information. The N_6 column gives the directly enumerated numbers of same-type simple base 6-cycles $(N_6(X), N_6(Z))$. This number is also relevant for the later lift design: each same-type base 6-cycle contributes one nonzero congruence constraint on the CPM exponents, so a larger N_6 can make the lift-label search harder even when the base-level certificates hold. The $N_{XZ}^{(2)}$ column gives the number of X -row/ Z -row pairs sharing two base columns. For every row, direct enumeration also checks that each X -row/ Z -row pair shares either

zero or two base columns, as required later for the CPM-lift orthogonality condition. The table certifies only the base-level properties covered by Theorems 2 and 3; it does not assert that the later lift constraints or decoding properties have been verified for those parameters. The gray special row is the $(3, 10)$ base over \mathbb{F}_{16} used for the 64-fold CPM lift; it is listed separately from the small-field row for the same (J, L) .

Table 1: Coefficient examples satisfying Proposition 1 over small finite fields for selected (J, L) . The gray special row is the \mathbb{F}_{16} base used for the 64-fold lift.

(J, L)	field	$ M $	actual parameters	$N_{XZ}^{(2)}$	N_6	coefficient arrays
(3, 6)	\mathbb{F}_7	3	[[42, 10, 3]]	189	(168, 168)	$\mathbf{a}^{(0)} = (0, 1, 3)$, $\mathbf{b}^{(0)} = (2, 4, 5)$, $\mathbf{a}^{(1)} = (0, 3, 1)$, $\mathbf{b}^{(1)} = (4, 2, 5)$
(3, 8)	\mathbb{F}_9	4	[[72, 22, 6]]	324	(432, 432)	$\mathbf{a}^{(0)} = (0, 1, 1 + \alpha)$, $\mathbf{b}^{(0)} = (2, 1 + 2\alpha, 2 + \alpha)$, $\mathbf{a}^{(1)} = (0, 1 + \alpha, 2)$, $\mathbf{b}^{(1)} = (\alpha, 2 + \alpha, 2 + 2\alpha)$
(3, 10)	\mathbb{F}_{11}	5	[[110, 48, 6]]	495	(880, 880)	$\mathbf{a}^{(0)} = (0, 1, 2)$, $\mathbf{b}^{(0)} = (3, 4, 5)$, $\mathbf{a}^{(1)} = (0, 2, 1)$, $\mathbf{b}^{(1)} = (4, 3, 5)$
(3, 10)	\mathbb{F}_{16}	5	[[160, 76, 4]]	720	(800, 800)	$\mathbf{a}^{(0)} = (0, 1, 2)$, $\mathbf{b}^{(0)} = (7, 3, 6)$, $\mathbf{a}^{(1)} = (8, 13, 2)$, $\mathbf{b}^{(1)} = (11, 10, 6)$
(3, 12)	\mathbb{F}_{13}	6	[[156, 82, 3]]	702	(1560, 1560)	$\mathbf{a}^{(0)} = (11, 6, 5)$, $\mathbf{b}^{(0)} = (12, 1, 9)$, $\mathbf{a}^{(1)} = (1, 4, 10)$, $\mathbf{b}^{(1)} = (2, 11, 7)$
(3, 14)	\mathbb{F}_{29}	7	[[406, 236, 6]]	1827	(2233, 2436)	$\mathbf{a}^{(0)} = (10, 25, 22)$, $\mathbf{b}^{(0)} = (24, 4, 14)$, $\mathbf{a}^{(1)} = (1, 25, 26)$, $\mathbf{b}^{(1)} = (18, 8, 14)$
(3, 16)	\mathbb{F}_{17}	8	[[272, 174, 6]]	1224	(3808, 3808)	$\mathbf{a}^{(0)} = (0, 1, 2)$, $\mathbf{b}^{(0)} = (3, 4, 5)$, $\mathbf{a}^{(1)} = (0, 3, 6)$, $\mathbf{b}^{(1)} = (5, 8, 11)$
(3, 18)	\mathbb{F}_{19}	9	[[342, 232, 6]]	1539	(5472, 5472)	$\mathbf{a}^{(0)} = (0, 1, 2)$, $\mathbf{b}^{(0)} = (3, 4, 5)$, $\mathbf{a}^{(1)} = (0, 2, 5)$, $\mathbf{b}^{(1)} = (10, 4, 7)$
(3, 20)	\mathbb{F}_{31}	10	[[620, 438, 6]]	2790	(7130, 7750)	$\mathbf{a}^{(0)} = (0, 1, 2)$, $\mathbf{b}^{(0)} = (3, 4, 5)$, $\mathbf{a}^{(1)} = (0, 5, 14)$, $\mathbf{b}^{(1)} = (6, 30, 20)$
(3, 30)	\mathbb{F}_{31}	15	[[930, 748, 6]]	4185	(26040, 26040)	$\mathbf{a}^{(0)} = (0, 1, 2)$, $\mathbf{b}^{(0)} = (3, 4, 5)$, $\mathbf{a}^{(1)} = (0, 3, 6)$, $\mathbf{b}^{(1)} = (11, 14, 4)$
(4, 8)	\mathbb{F}_{13}	4	[[104, 6, 12]]	832	(1456, 1456)	$\mathbf{a}^{(0)} = (0, 1, 6, 5)$, $\mathbf{b}^{(0)} = (12, 9, 10, 7)$, $\mathbf{a}^{(1)} = (0, 10, 12, 2)$, $\mathbf{b}^{(1)} = (8, 9, 3, 4)$
(4, 10)	\mathbb{F}_{11}	5	[[110, 28, 10]]	880	(3520, 3520)	$\mathbf{a}^{(0)} = (9, 8, 1, 4)$, $\mathbf{b}^{(0)} = (7, 3, 0, 6)$, $\mathbf{a}^{(1)} = (5, 10, 7, 3)$, $\mathbf{b}^{(1)} = (6, 9, 2, 0)$
(4, 12)	\mathbb{F}_{13}	6	[[156, 58, 8]]	1248	(6240, 6240)	$\mathbf{a}^{(0)} = (6, 4, 2, 8)$, $\mathbf{b}^{(0)} = (10, 11, 3, 0)$, $\mathbf{a}^{(1)} = (9, 8, 4, 0)$, $\mathbf{b}^{(1)} = (6, 1, 5, 11)$
(4, 14)	\mathbb{F}_{29}	7	[[406, 180, $d \geq 9$]]	3248	(8526, 9744)	$\mathbf{a}^{(0)} = (0, 1, 17, 13)$, $\mathbf{b}^{(0)} = (25, 5, 20, 10)$, $\mathbf{a}^{(1)} = (0, 28, 13, 15)$, $\mathbf{b}^{(1)} = (23, 5, 16, 12)$
(4, 16)	\mathbb{F}_{17}	8	[[272, 142, 8]]	2176	(15232, 15232)	$\mathbf{a}^{(0)} = (0, 1, 14, 10)$, $\mathbf{b}^{(0)} = (11, 13, 5, 9)$, $\mathbf{a}^{(1)} = (0, 6, 16, 13)$, $\mathbf{b}^{(1)} = (11, 1, 7, 4)$
(4, 18)	\mathbb{F}_{19}	9	[[342, 196, $9 \leq d \leq 10$]]	2736	(21888, 21888)	$\mathbf{a}^{(0)} = (0, 1, 18, 17)$, $\mathbf{b}^{(0)} = (9, 12, 10, 11)$, $\mathbf{a}^{(1)} = (0, 12, 11, 8)$, $\mathbf{b}^{(1)} = (6, 10, 18, 7)$
(4, 20)	\mathbb{F}_{31}	10	[[620, 378, $9 \leq d \leq 10$]]	4960	(29140, 29450)	$\mathbf{a}^{(0)} = (0, 1, 29, 27)$, $\mathbf{b}^{(0)} = (10, 8, 25, 7)$, $\mathbf{a}^{(1)} = (0, 26, 28, 14)$, $\mathbf{b}^{(1)} = (21, 2, 12, 19)$
(4, 22)	\mathbb{F}_{23}	11	[[506, 328, $9 \leq d \leq 10$]]	4048	(40480, 40480)	$\mathbf{a}^{(0)} = (0, 1, 9, 22)$, $\mathbf{b}^{(0)} = (16, 7, 12, 21)$, $\mathbf{a}^{(1)} = (0, 22, 20, 12)$, $\mathbf{b}^{(1)} = (4, 7, 13, 10)$
(4, 24)	\mathbb{F}_{37}	12	[[888, 598, 8]]	7104	(51060, 51948)	$\mathbf{a}^{(0)} = (0, 1, 26, 17)$, $\mathbf{b}^{(0)} = (3, 12, 35, 14)$, $\mathbf{a}^{(1)} = (0, 7, 13, 18)$, $\mathbf{b}^{(1)} = (24, 21, 25, 11)$
(4, 26)	\mathbb{F}_{53}	13	[[1378, 960, $d \geq 7$]]	11024	(60632, 68900)	$\mathbf{a}^{(0)} = (0, 1, 49, 2)$, $\mathbf{b}^{(0)} = (4, 20, 12, 11)$, $\mathbf{a}^{(1)} = (0, 11, 21, 51)$, $\mathbf{b}^{(1)} = (43, 31, 22, 4)$
(4, 28)	\mathbb{F}_{29}	14	[[812, 586, 8]]	6496	(84448, 84448)	$\mathbf{a}^{(0)} = (0, 1, 8, 24)$, $\mathbf{b}^{(0)} = (15, 11, 28, 17)$, $\mathbf{a}^{(1)} = (0, 26, 23, 12)$, $\mathbf{b}^{(1)} = (18, 8, 28, 19)$
(4, 30)	\mathbb{F}_{31}	15	[[930, 688, $d \geq 7$]]	7440	(104160, 104160)	$\mathbf{a}^{(0)} = (0, 1, 11, 6)$, $\mathbf{b}^{(0)} = (23, 19, 17, 14)$, $\mathbf{a}^{(1)} = (0, 17, 8, 10)$, $\mathbf{b}^{(1)} = (23, 2, 21, 20)$
(5, 10)	\mathbb{F}_{11}	5	[[110, 8, 12]]	1375	(8800, 8800)	$\mathbf{a}^{(0)} = (4, 3, 9, 6, 2)$, $\mathbf{b}^{(0)} = (1, 0, 10, 8, 5)$, $\mathbf{a}^{(1)} = (8, 6, 10, 2, 7)$, $\mathbf{b}^{(1)} = (4, 5, 3, 9, 1)$

The $(3, 30)$ row gives a $J = 3$ base whose design-rate lower bound is $1 - 2J/L = 1 - 6/30 = 0.8$. It is the smallest such row within this two-branch certificate: the condition $1 - 2J/L \geq 0.8$ with $J = 3$ forces $L \geq 30$, hence $|M| = L/2 \geq 15$, and the same-type disjointness certificate requires at least two nonzero M -cosets, so $q - 1 \geq 2|M| \geq 30$. Thus $q \geq 31$, and the displayed \mathbb{F}_{31} example attains the minimum possible field size and base length $n = 2q|M| = 930$ under these certificate conditions.

2.4 Zero Congruence Constraints for Orthogonality

This subsection states the condition that preserves CSS orthogonality when a base pair is replaced by a P -fold circulant permutation matrix (CPM) lift. The condition is a zero congruence constraint on the CPM exponents. The base-side hypothesis in Theorem 4 is not merely that each binary

inner product is even. It requires every X -row and Z -row to share either zero or two base columns. If two columns are shared, the two CPM blocks can be made identical and hence cancel over \mathbb{F}_2 . If four or more columns are shared, the binary base inner product is still zero, but a different condition is needed to cancel a sum of more than two CPM blocks. The $N_{XZ}^{(2)}$ column in Table 1 records the direct check of this hypothesis for each listed base.

Theorem 4 (CSS Orthogonality after CPM Lifting). Let (H_X, H_Z) be a binary base-matrix pair. Assume that every X -row and Z -row share either zero or two base columns. In a P -fold CPM lift, assign

$$s_X(r, c), s_Z(z, c) \in \mathbb{Z}/P\mathbb{Z}$$

to every nonzero X -edge (r, c) and Z -edge (z, c) , and replace the corresponding nonzero entries by $\Pi^{s_X(r,c)}$ and $\Pi^{s_Z(z,c)}$. Here Π^s is the $P \times P$ CPM whose nonzero entry in row u is in column $u + s$. If an X -row r and a Z -row z share exactly two base columns c_0, c_1 , assume that

$$s_X(r, c_0) - s_Z(z, c_0) \equiv s_X(r, c_1) - s_Z(z, c_1) \pmod{P} \quad (10)$$

for every such pair. Then the lifted matrices satisfy

$$H_X^{\text{lift}}(H_Z^{\text{lift}})^\top = 0.$$

□

Proof. If X -row r and Z -row z share no base column, the corresponding lifted block inner product is zero. If they share base columns c_0, c_1 , the lifted block inner product over \mathbb{F}_2 is

$$\Pi^{s_X(r,c_0) - s_Z(z,c_0)} + \Pi^{s_X(r,c_1) - s_Z(z,c_1)}.$$

Condition (10) makes the two CPMs identical, so their sum over \mathbb{F}_2 is zero. Thus every lifted X -row/ Z -row block inner product is zero, and $H_X^{\text{lift}}(H_Z^{\text{lift}})^\top = 0$ follows. □

Equation (10) is a homogeneous linear congruence in the CPM exponents. If all base-edge labels are collected into a vector \mathbf{s} , the lift-orthogonality constraints have the form

$$A_0 \mathbf{s} = \mathbf{0} \pmod{P}.$$

2.5 Nonzero Congruence Constraints for 6-Cycle Exclusion

We next state the condition that prevents a same-type base 6-cycle from closing after the lift while preserving the zero congruence constraints for orthogonality. For each base 6-cycle γ , 6-cycle exclusion requires a linear form $\ell_\gamma(\mathbf{s})$ in the CPM exponents to satisfy

$$\ell_\gamma(\mathbf{s}) \neq 0 \pmod{P}.$$

The method for finding labels that satisfy both zero and nonzero congruence constraints is described in Section 2.7.

The next theorem is independent of the finite-field realization of the base. Once the base has no same-type 4-cycles, a same-type lifted 6-cycle can appear from a base 6-cycle only when the corresponding signed CPM-exponent sum is zero. Thus removing all lifted 6-cycles amounts to imposing one nonzero congruence constraint for each same-type base 6-cycle. When N_6 is large, these nonzero constraints may substantially restrict the remaining choices of lift labels, and satisfiability is a separate finite check rather than a consequence of the base construction alone.

Theorem 5 (CPM Lift Condition for Avoiding Lifted 6-Cycles). Fix one side $S \in \{X, Z\}$ and let H_S be a binary base matrix whose Tanner graph has no 4-cycles. For $s \in \mathbb{Z}/P\mathbb{Z}$, let Π^s be the $P \times P$ CPM whose nonzero entry in row u is in column $u + s$, with indices read modulo P . Construct a P -fold CPM lift H_S^{lift} of H_S by replacing each nonzero base entry, equivalently each base edge (r, c) , by $\Pi^{s_S(r,c)}$, where

$$s_S(r, c) \in \mathbb{Z}/P\mathbb{Z}.$$

Thus lifted check (r, u) is incident to lifted variable $(c, u + s_S(r, c))$. For a base 6-cycle

$$r_0 - c_0 - r_1 - c_1 - r_2 - c_2 - r_0,$$

define its signed CPM-exponent sum by

$$\begin{aligned} \Delta_S = & (s_S(r_0, c_0) - s_S(r_1, c_0)) + (s_S(r_1, c_1) - s_S(r_2, c_1)) \\ & + (s_S(r_2, c_2) - s_S(r_0, c_2)) \pmod{P}. \end{aligned}$$

This base 6-cycle closes to a length-6 cycle in the lifted Tanner graph if and only if $\Delta_S = 0$. Consequently, if $\Delta_S \neq 0$ for every same-type base 6-cycle on side S , then the lifted side- S Tanner graph has girth at least 8. \square

Proof. Follow a lifted walk above the displayed base cycle, starting at lifted check (r_0, u) . In the CPM block at (r_0, c_0) , the nonzero entry in row coordinate u is in column coordinate $u + s_S(r_0, c_0)$. Thus the walk reaches variable $(c_0, u + s_S(r_0, c_0))$. To continue through the CPM block at (r_1, c_0) , the next lifted check coordinate must be

$$u + s_S(r_0, c_0) - s_S(r_1, c_0).$$

Continuing the same calculation along the six CPM blocks changes the lifted check coordinate by exactly Δ_S . Therefore the lifted walk returns to the starting lifted check coordinate if and only if $\Delta_S = 0$. This is the standard cycle condition for cyclic graph lifts [4].

Because H_S has no base 4-cycles, replacing nonzero entries by CPM blocks cannot create lifted 4-cycles unless a base 4-cycle exists. If all base 6-cycles have nonzero signed CPM-exponent sum, no 6-cycle closes in the lift. Therefore the lifted side- S Tanner graph has no cycles of length 4 or 6, and its girth is at least 8. \square

2.6 Nonzero Congruence Constraints for Low-Weight Lift Supports

We first fix the terminology. In a P -fold CPM lift, a base column c is replaced by the P lifted columns

$$(c, u), \quad u \in \mathbb{Z}/P\mathbb{Z}.$$

We call this the lifted column set associated with c .

Let $K \leq \mathbb{Z}/P\mathbb{Z}$ be a subgroup. Fix a base-column support T , and choose a representative $f_c \in \mathbb{Z}/P\mathbb{Z}$ for each $c \in T$. The lifted support

$$\tilde{T}(\mathbf{f}, K) = \{(c, f_c + k) : c \in T, k \in K\}$$

is called the lift-coordinate coset lift support with base support T , lift-coordinate subgroup K , and representative vector $\mathbf{f} = (f_c)_{c \in T}$. It uses one coset $f_c + K$ among the lift coordinates over each base column c , rather than all P lifted columns associated with c . Its weight is therefore $|T||K|$. From the construction viewpoint, this definition separates two choices. The base support T specifies which base columns are used, while \mathbf{f} specifies which lift coordinates are used after lifting. If a base-stage support satisfies

$$H_X \mathbf{1}_T = \mathbf{0}$$

and is not generated by Z -check rows, it can become a Z -type logical-operator candidate. However, the base support is only the projection of a lifted support. For a lift-coordinate coset support, the corresponding lifted equation is

$$H_X^{\text{lift}} \mathbf{1}_{\tilde{T}(\mathbf{f}, K)} = \mathbf{0}.$$

To become a genuine low-weight lifted support, this lifted equation must hold for some choice of representatives f_c .

Thus removing lifted 6-cycles is not the only finite-length constraint needed after the base has been fixed. One must also check specified small base-support families \mathcal{O} and small lift-coordinate subgroups K . In the (3, 10) instance below, the relevant base support has eight base columns and uses a two-point coset over each base column, giving a lifted candidate of weight 16.

The following theorem states only a necessary condition for this type of lift-coordinate coset support to have zero X -syndrome. It does not characterize all logical operators. How this necessary condition is used in lift design is explained after the theorem.

Theorem 6 (Necessary Condition for a Lift-Coordinate Coset Support to Have Zero Syndrome). Let (H_X, H_Z) be a binary CSS base pair. For $s \in \mathbb{Z}/P\mathbb{Z}$, let Π^s be the $P \times P$ CPM whose nonzero entry in row u is in column $u + s$. Let H_X^{lift} be the P -fold CPM lift of H_X obtained by replacing each nonzero X -edge (r, c) by $\Pi^{s_X(r, c)}$, where

$$s_X(r, c) \in \mathbb{Z}/P\mathbb{Z}.$$

Let $K \leq \mathbb{Z}/P\mathbb{Z}$ be a subgroup. Fix a base-column support T , and consider lifted supports of the form

$$\tilde{T}(\mathbf{f}, K) = \{(c, f_c + k) : c \in T, k \in K\}, \quad f_c \in \mathbb{Z}/P\mathbb{Z}.$$

If

$$H_X^{\text{lift}} \mathbf{1}_{\tilde{T}(\mathbf{f}, K)} = \mathbf{0},$$

then for each X -row r whose intersection with T contains exactly two columns a, b ,

$$f_b - f_a \equiv s_X(r, b) - s_X(r, a) \quad \text{in } (\mathbb{Z}/P\mathbb{Z})/K \tag{11}$$

is necessary. □

Proof. In the CPM block $\Pi^{s_X(r, c)}$, lifted check coordinate u is adjacent to lifted variable coordinate

$$v = u + s_X(r, c).$$

Equivalently, the lifted check coordinate reached from (c, v) through edge (r, c) is $u = v - s_X(r, c)$. If r meets T exactly in a, b , then the lifted support gives the two lifted-check-coordinate cosets

$$f_a + K - s_X(r, a), \quad f_b + K - s_X(r, b).$$

For the lifted syndrome to vanish at this row, these two cosets must be equal. This equality is equivalent to (11) in the quotient group $(\mathbb{Z}/P\mathbb{Z})/K$. Thus the displayed equation is necessary for the prescribed pattern to have a zero-syndrome lift. □

The next example explains how the finite consistency test in Theorem 6 is used for the selected lift. It records a concrete support family that is excluded; it is not a proof that every weight-16 logical operator is absent.

Example 2 (Excluding a Two-Point Lift-Coordinate Coset Pattern in the 64-Fold Lift). In the (3, 10) construction considered here, the candidate to be excluded has eight base columns and places two lift-coordinate values over each base column. Take

$$P = 64, \quad K = \{0, 32\} \leq \mathbb{Z}/64\mathbb{Z},$$

and, for example,

$$T_0 = \{10, 25, 55, 60, 99, 104, 134, 149\}.$$

This is not an isolated support. Together with the paired seed

$$T_1 = \{15, 20, 50, 65, 94, 109, 139, 144\},$$

translations in the finite field and scalings by the subgroup used in this construction generate 20 distinct base supports of this form after duplicates are removed. For each support, the relevant X -row graph is connected. Thus, if the quotient congruences below are consistent, the representatives $f_c \bmod 32$ are determined up to a global translation. Consequently, one closing base support would give 32 lifted supports of weight 16. The lift-coordinate coset support on T_0 has the form

$$\{(c, f_c), (c, f_c + 32) : c \in T_0\},$$

so its weight is $8 \cdot 2 = 16$. Since $(\mathbb{Z}/64\mathbb{Z})/K$ is naturally identified with $\mathbb{Z}/32\mathbb{Z}$, each X -row meeting T_0 in exactly two columns a, b gives the necessary congruence

$$f_b - f_a \equiv s_X(r, b) - s_X(r, a) \pmod{32}.$$

Thus the exclusion check is a finite consistency test on the unknowns $f_c \bmod 32$. If the congruences around the rows touching T_0 are inconsistent, then no choice of representatives f_c can make this two-point lift-coordinate coset pattern have zero X -syndrome. The same test is applied to all 20 supports in the orbit. For the selected 64-fold lift, all 20 systems are inconsistent. This excludes the specified weight-16 Z -type lift-coordinate coset pattern, but it does not by itself prove that all weight-16 logical operators are absent. \square

The theorem converts a specified low-weight lift-support pattern into finite linear constraints on lift labels. For a fixed base support T , form the constraint graph obtained from (11): its vertices are the columns in T , and each X -row meeting T in exactly two columns gives an edge between them. Adding the equations around a cycle η in this graph cancels the f_c terms. Thus the necessary condition includes a zero congruence

$$\ell_{T,\eta}(\mathbf{s}) = 0 \quad \text{in } (\mathbb{Z}/P\mathbb{Z})/K.$$

To exclude the specified support, it is enough to choose labels for which at least one such cycle satisfies

$$\ell_{T,\eta}(\mathbf{s}) \neq 0 \quad \text{in } (\mathbb{Z}/P\mathbb{Z})/K.$$

In this sense, exclusion of a specified low-weight lift support can also be handled as a nonzero congruence constraint on the lift labels.

2.7 Label Search Satisfying Zero and Nonzero Congruence Constraints

The previous subsections express the lift-label requirements as congruence constraints. Orthogonality gives zero congruence constraints

$$A_0 \mathbf{s} = \mathbf{0} \pmod{P},$$

whereas 6-cycle exclusion and specified low-weight lift-support exclusion give nonzero congruence constraints of the form

$$\ell_j(\mathbf{s}) \neq 0 \pmod{m_j}.$$

Here $m_j = P$ for 6-cycle exclusion, while for lift-coordinate coset support exclusion, $m_j = |(\mathbb{Z}/P\mathbb{Z})/K|$ after identifying the quotient group with $\mathbb{Z}/m_j\mathbb{Z}$.

The search is a finite congruence-satisfaction problem. First, all CPM exponents on base edges are collected as unknowns, and the zero congruence system $A_0 \mathbf{s} = \mathbf{0}$ from orthogonality is solved.

Keeping this solution set, the nonzero congruence constraints are tested one by one. When a violated constraint $\ell_j(\mathbf{s}) = 0$ is found, a nonzero value $u_j \in \mathbb{Z}/m_j\mathbb{Z}$ is selected and the linear congruence

$$\ell_j(\mathbf{s}) = u_j \pmod{m_j}$$

is added. If the enlarged linear system becomes inconsistent, another nonzero value is tried or the previous choice is backtracked. This iteration avoids the zero sets of the nonzero constraints while always remaining inside the orthogonality solution set.

The implementation uses random nonzero values and restarts. Since the candidate values for each u_j are finite, the procedure can be made complete by backtracking over all candidates. Therefore, as long as only finitely many zero and nonzero congruence constraints are considered, the complete version finds a solution whenever one exists. For the adopted labels, all zero and nonzero congruence constraints are directly rechecked after the search, independently of the search history.

2.8 Testing Distance Upper-Bound Witnesses

Lift constraints exclude short cycles and specified low-weight support patterns. By contrast, an upper bound on the minimum distance of the constructed finite-length code is obtained by finding an explicit logical representative and verifying that it is not a stabilizer. The next theorem states this test for a general CSS check-matrix pair. Here a witness means a non-stabilizer logical representative whose kernel condition and row-space nonmembership have both been directly verified. It is evidence for an upper bound, not a determination of the exact distance.

Theorem 7 (Testing Distance Upper-Bound Witnesses). Let (H_X, H_Z) be a binary CSS check-matrix pair. If a column set S_X satisfies

$$\mathbf{1}_{S_X} \in \ker H_Z, \quad \mathbf{1}_{S_X} \notin \text{row}(H_X),$$

then the corresponding CSS code satisfies

$$d_X \leq |S_X|.$$

Similarly, if a column set S_Z satisfies

$$\mathbf{1}_{S_Z} \in \ker H_X, \quad \mathbf{1}_{S_Z} \notin \text{row}(H_Z),$$

then

$$d_Z \leq |S_Z|.$$

If both witnesses are available, then

$$d \leq \min\{|S_X|, |S_Z|\}.$$

□

Proof. The condition $\mathbf{1}_{S_X} \in \ker H_Z$ says that S_X is a candidate X -type logical representative. The condition $\mathbf{1}_{S_X} \notin \text{row}(H_X)$ says that this representative is not an X -stabilizer. Thus a nontrivial X -type logical representative of weight $|S_X|$ exists, and $d_X \leq |S_X|$. The same argument gives $d_Z \leq |S_Z|$ for a Z -type witness. Since $d = \min(d_X, d_Z)$, the final claim follows. □

This verification rule is the same logical-witness test used in [26]. It is separate from Theorem 6. Theorem 6 excludes specified low-weight support patterns, whereas Theorem 7 gives an upper bound by directly checking explicit logical representatives on the constructed matrices.

3 Concrete Example of Section 2: the \mathbb{F}_{16} Base and 64-Fold Lift Constraints

We now specialize the general construction and lift constraints from Section 2 to the instance used in this paper. We fix the $(3, 10)$ base over \mathbb{F}_{16} shown as the gray special row in Table 1, and then state the conditions imposed on the 64-fold CPM lift. The base-stage coefficients, base parameters, and same-type base 6-cycle counts are recorded in the table. The following subsections correspond to Sections 2.4–2.7: zero congruence constraints for orthogonality, nonzero congruence constraints for 6-cycle exclusion, nonzero congruence constraints for low-weight lift-support exclusion, and the label search satisfying all of them.

The table states the selected \mathbb{F}_{16} coefficients and records that the base has 800 same-type simple 6-cycles on each side. At the lift stage, the degree, commutation, and same-type 4-cycle conditions are already fixed at the base level. The remaining finite-length checks are therefore to keep CSS orthogonality after CPM lifting, make each same-type base 6-cycle nonclosing, and exclude the specified weight-16 logical-support orbit.

3.1 Concrete Zero Congruence Constraints for Orthogonality

Corresponding to Section 2.4, we first specialize the zero congruence constraints that preserve CSS orthogonality after the 64-fold lift. The base construction gives CSS orthogonality by making every X -row and Z -row share either zero or two base columns. However, orthogonality after CPM lifting also depends on the labels. If an X -row r and a Z -row z share base columns c_0, c_1 , the lifted block inner product is

$$\prod^{s_X(r, c_0) - s_Z(z, c_0)} + \prod^{s_X(r, c_1) - s_Z(z, c_1)}.$$

This sum is zero over \mathbb{F}_2 if and only if

$$s_X(r, c_0) - s_Z(z, c_0) \equiv s_X(r, c_1) - s_Z(z, c_1) \pmod{64}.$$

Thus the lift-label search imposes no condition on X -row/ Z -row pairs with no shared base column, and imposes the displayed congruence on all pairs sharing two base columns. For the selected 64-fold labels, this congruence holds for all 720 paired X - Z overlaps, so $H_X^{\text{lift}}(H_Z^{\text{lift}})^T = 0$ is preserved.

3.2 Concrete Nonzero Congruence Constraints for 6-Cycle Exclusion

After the base construction, the remaining short-cycle condition concerns the same-type 6-cycles. The CPM lift is not used to repair commutation or row weights; those properties have already been settled at the base stage. The general acceptance condition is Theorem 5: every same-type base 6-cycle must have nonzero signed CPM-exponent sum. The base has 800 same-type simple 6-cycles on each of the X and Z sides.

This requirement is satisfied by the 64-fold CPM lift used below. The liftability verification over both \mathbb{F}_2 and \mathbb{F}_{997} found that all 800 same-type 6-cycles are avoidable and that no 6-cycle is forced to close. For the selected 64-fold labels, no base 6-cycle has zero signed CPM-exponent sum, so no same-type 6-cycle closes in the lifted graph.

The base length is 160, so the 64-fold lift has length $N = 10240$ and 3072 rows on each side. It remains $(3, 10)$ -regular on both sides and satisfies the CSS condition. For the selected labels, the number of lifted same-type 6-cycles arising from base 6-cycles is zero on both the X and Z sides.

3.3 Concrete Low-Weight Lift-Support Exclusion

Avoiding lifted 6-cycles alone does not prevent the minimum distance from becoming small. Even among lifts in which no same-type base 6-cycle closes, many candidates can appear that become

weight-16 Z -type logical operators after lifting. They arise when a small support of eight base columns is placed on two lift-coordinate values over each base column. Thus the next finite-length support pattern to exclude is the following weight-16 logical orbit.

This orbit is obtained at the base stage by looking for small supports in $\ker H_X$ that are not in $\text{row}(H_Z)$, and then closing the resulting candidates under the symmetries of the \mathbb{F}_{16} instance. The two seed supports are

$$T_0 = \{10, 25, 55, 60, 99, 104, 134, 149\}$$

and

$$T_1 = \{15, 20, 50, 65, 94, 109, 139, 144\}.$$

Both lie in $\ker H_X$ but not in $\text{row}(H_Z)$. If they close in the lift, they produce pure Z -type nondegenerate logical operators. The forbidden lifted pattern places a two-point lift-coordinate coset $\{f, f + 32\}$ over each base column. Since each seed support has eight base columns, this pair pattern has total weight 16.

These two supports generate the full family considered here. By “orbit” we mean the 20 distinct supports obtained from them, after duplicate supports are removed, by translations in \mathbb{F}_{16} , scalings by M , and the two orientations. All 20 lie in $\ker H_X$ and outside $\text{row}(H_Z)$. Thus closure of this orbit in the lift would produce a weight-16 Z -type nondegenerate logical operator.

The exclusion uses Theorem 6 with $P = 64$ and $K = \{0, 32\}$. For each support, if the congruence system in Theorem 6 is inconsistent, then that support cannot occur as a two-point lift-coordinate coset pattern in the lift. For the selected 64-fold lift, this test excludes all 20 supports in the orbit. This is a sufficient certificate for the specified orbit pattern; it is not a characterization of all possible low-weight logical operators.

3.4 Concrete Label Search and Accepted Instance

For the selected 64-fold labels, we directly rechecked all zero congruence constraints for orthogonality, all nonzero congruence constraints for same-type base 6-cycles, and all nonzero congruence constraints for the 20 weight-16 base supports. Thus CSS orthogonality, nonclosure of same-type lifted 6-cycles, and exclusion of the specified weight-16 lift-coordinate coset pattern hold simultaneously.

The \mathbb{F}_2 ranks are

$$\text{rank}(H_X^{\text{lift}}) = 3066, \quad \text{rank}(H_Z^{\text{lift}}) = 3066.$$

Thus the effective 64-fold-lift code parameters are

$$[[10240, 4108]],$$

with rate

$$R = 4108/10240 = 0.401171875.$$

In frame error rate (FER) plots we also use the regular $(3, 10)$ design rate $R = 0.4$ as a reference; this is close to, but distinct from, the finite-length effective rank.

The girth certificate gives a first rigorous lower bound on the CSS distance, but the finite-length matrices allow a stronger direct certificate. The support enumeration used here orders a candidate by its smallest column, maintains the current syndrome, and prunes a branch whenever the unsatisfied checks require more new columns than the target weight allows. Applied to both lifted check matrices, this complete enumeration found no nonzero vector of weight at most 9 in either kernel. This computation is separate from the weight-16 orbit exclusion: it gives a certified lower bound below weight 10, whereas the orbit condition excludes one specified weight-16 support family.

Proposition 2 (Certified distance lower bound). For the 64-fold lift constructed here,

$$d_X \geq 10, \quad d_Z \geq 10, \quad d \geq 10.$$

□

Proof. Every X -type logical representative is a nonzero vector in $\ker H_Z$, and every Z -type logical representative is a nonzero vector in $\ker H_X$. The complete support enumeration described above found no nonzero vector of weight at most 9 in either kernel. Therefore every nonzero X -type or Z -type logical representative has weight at least 10. Since $d = \min(d_X, d_Z)$, the stated CSS distance lower bound follows. □

The same idea gives a precise way to turn the construction into a larger certified-distance construction. The key point is that a lower bound on the CSS distance is not obtained from decoder screening alone; it must be certified by excluding all nontrivial logical representatives below the target weight. The following acceptance criterion is the finite-length condition that has to be added to a lift search when a larger lower bound is required.

Proposition 3 (Target-distance acceptance criterion). Fix a target integer D . For a lifted CSS pair (H_X, H_Z) , suppose that exact finite enumeration verifies

$$\{\mathbf{x} \in \ker H_Z : 1 \leq \text{wt}(\mathbf{x}) < D\} \subseteq \text{row}(H_X)$$

and

$$\{\mathbf{z} \in \ker H_X : 1 \leq \text{wt}(\mathbf{z}) < D\} \subseteq \text{row}(H_Z).$$

Then the corresponding CSS code satisfies

$$d_X \geq D, \quad d_Z \geq D, \quad d \geq D.$$

□

Proof. The first inclusion says that every X -type kernel vector of weight below D is an X stabilizer, so no nontrivial X logical representative has weight below D . Hence $d_X \geq D$. The second inclusion gives the same statement for Z -type representatives, hence $d_Z \geq D$. Taking the minimum gives $d \geq D$. □

This proposition is a constructive acceptance rule: in a search for lift labels, one can reject a candidate lift unless it passes the two exact inclusions for the chosen target D . The present 64-fold lift has been certified with the stronger condition that both kernels contain no nonzero vector of weight at most 9, so it realizes Proposition 3 with $D = 10$. Larger certified lower bounds require completing the same exact finite enumeration for the larger target D ; decoder failures or defect-focused screening by themselves are not used as distance lower-bound certificates.

We also record an explicit distance upper-bound certificate for the same finite-length code. This step has a different purpose from the orbit exclusion above. It does not identify the exact distance; it only records explicit logical representatives whose status has been verified exactly. Following the acceptance criterion in [26], a candidate is used only after two binary checks: membership in the kernel of the opposite check matrix and exclusion from the corresponding stabilizer row space. In this paragraph, a witness means such a verified non-stabilizer logical representative; it is evidence for an upper bound, not for an exact distance value. The lift-coordinate coset exclusion condition in Theorem 6 is used to rule out a specified low-weight support family. By contrast, the following upper-bound witnesses are not consequences of that exclusion criterion; they are verified directly on the constructed lifted matrices by checking kernel membership and nonmembership in the relevant stabilizer row spaces.

Proposition 4 (Certified distance upper bound). For the 64-fold lift constructed here,

$$d_X \leq 32, \quad d_Z \leq 32, \quad d \leq 32.$$

□

Proof. For lifted columns, write (c, f) for the column $64c + f$, where c is a base column and $f \in \mathbb{Z}/64\mathbb{Z}$. Let $K = 16\mathbb{Z}/64\mathbb{Z} = \{0, 16, 32, 48\}$. For the X -type representative, take

$$\tilde{S}_X = \{(c, r + k) : (c, r) \in A_X, k \in K\},$$

where

$$A_X = \{(27, 12), (37, 3), (62, 1), (72, 5), (83, 2), (93, 6), (128, 5), (138, 12)\}.$$

This support has weight $8 \cdot 4 = 32$. Direct binary verification on the 64-fold matrices gives

$$\mathbf{1}_{\tilde{S}_X} \in \ker H_Z, \quad \mathbf{1}_{\tilde{S}_X} \notin \text{row}(H_X).$$

Thus $d_X \leq 32$.

For the Z -type representative, take

$$\tilde{S}_Z = \{(c, r + k) : (c, r) \in A_Z, k \in K\},$$

where

$$A_Z = \{(64, 7), (69, 3), (74, 12), (79, 8), (81, 7), (86, 7), (91, 14), (96, 4)\}.$$

This support has weight $8 \cdot 4 = 32$, and direct binary verification gives

$$\mathbf{1}_{\tilde{S}_Z} \in \ker H_X, \quad \mathbf{1}_{\tilde{S}_Z} \notin \text{row}(H_Z).$$

Thus $d_Z \leq 32$. Since the CSS distance is $d = \min(d_X, d_Z)$, $d \leq 32$. □

Combining the lower and upper bounds, the present certificates give

$$10 \leq d_X \leq 32, \quad 10 \leq d_Z \leq 32, \quad 10 \leq d \leq 32.$$

They do not determine the exact lifted distance.

4 Decoder: Joint Log-Domain BP and Low-Complexity Post-Processing

This section specifies the finite-length decoding procedure used for the constructed 64-fold lift. It records the joint log-domain belief-propagation setting, the standard decoder parameters, and the post-processing rules used when a small residual syndrome remains. The point of the section is to make the subsequent FER measurements reproducible as decoder measurements, separate from the construction certificates.

The construction certificates address graph structure and one known low-weight logical-support pattern. The decoding experiment is a separate finite-length question: how this verified lifted code behaves under joint BP and deterministic post-processing. The BP decoder used here is joint BP in the binary factor-graph formulation of CSS syndrome decoding [29]. The choice to record small residual syndromes and post-processing outcomes follows the finite-length viewpoint that low-probability failures can be dominated by small trapping or logical structures rather than by the average ensemble behavior alone [9, 30, 26]. The implementation is the log-domain version: messages are stored and updated as log-likelihood ratios, which avoids probability underflow and

gives numerically stable check-node and variable-node updates. For the depolarizing channel, joint BP keeps the local correlation between the two Pauli error components through the joint prior at each qubit. The purpose of the post-processing is to decide whether a residual syndrome has a small-neighborhood explanation visible from the joint-BP output and the lifted Tanner graph. The decoder uses

$$\text{row degree} = 10, \quad \text{column degree} = 3$$

for the present matrices. The standard parameters are

$$\text{iters} = 1000, \quad \text{damping} = 0.3.$$

If BP does not converge to the target syndrome, a fallback run with zero damping is attempted.

Table 2 summarizes the post-processing rules. They do not use the true error; they use only the visible syndrome, log-likelihood ratios, hard-decision sequence, and the lift structure. The active rules are deliberately low-complexity post-processing rules: local linear solves on decoder-visible candidate sets, prefix-size searches over suspicious bits, flip-history candidates, short-path closures, single-column repairs, syndrome-2 core repairs, and exact or beam-style searches only for residual syndromes with one to four unsatisfied checks. We do not run a global low-weight syndrome solver over all qubits as part of the reported decoder. We do not count any post-hoc logical-bank correction as decoder post-processing. Such a correction can be constructed in a replay analysis by comparing a syndrome-valid decoder output with the saved true error, extracting the residual nontrivial logical operator, and adding that same operator back to the same recorded failure. This uses information obtained from the failure being corrected. It is therefore used only to diagnose failure types or to certify an upper bound on the minimum distance, and it is not included in the FER measurements reported below. For syndrome-2 residuals, we additionally look for small error-trapping-set core patterns. Here “core” means the induced small residual subgraph pattern used by the repair rule. When only one to four unsatisfied checks remain, we switch to an exact or beam-style search on decoder-visible candidate sets, mainly the corresponding small Tanner neighborhood. Thus the implemented rule is local: it is meant to repair small residual syndromes that have a low-weight explanation visible from the BP output and the lift graph. A small residual weight measured later by comparing with the saved true error is evidence that a stronger global low-weight syndrome solver could repair the replay case, but it is not itself information available to the decoder.

Table 2: Post-processing rules used after belief propagation. The active rules use only the decoder output, the syndrome, the log-likelihood ratios, and the lift structure. The final row records a replay-only diagnostic that is explicitly excluded from the decoder.

Rule	Main target	Description
Local linear solve	Small residual unsatisfied syndromes	Collects low-LLR bits near the unsatisfied checks and solves the induced linear system on that candidate set. This is the default first post-processing step.
Prefix-size search	Unknown suspicious-set size	Orders all bits by suspiciousness and uses bisection to find the smallest prefix size K for which the syndrome difference is solvable.
Diagnostic prefix search	Boundary between unique and non-unique local solutions	Extends the prefix-size search by probing the transition between unique and non-unique local solution regimes.
Flip-history candidate set	Oscillatory BP trajectories	Uses the bits whose hard decisions flipped during BP iterations as the candidate set. If this history set is insufficient, it falls back to a lightweight OSD step.
Path-based closure	Short lifted paths between residual checks	Builds a candidate set from short paths connecting residual unsatisfied checks and from the closure around those paths.
Common-column correction	Three unsatisfied checks explained by one column	If three unsatisfied checks are incident to a common column, this method cancels the syndrome by flipping that single bit.
Syndrome-2 core repair	Syndrome-2 error-trapping-set cores	Matches a two-unsatisfied residual against lifted error-trapping-set templates and repairs it using the corresponding core support.
Small-residual exact search	Only one to four unsatisfied checks remain	Runs an exact or beam-style search on decoder-visible candidate sets, mainly small Tanner neighborhoods, to find a low-weight correction that cancels the small residual syndrome. This is not a global low-weight syndrome solver, so a replay case can still remain failed even if the residual against the saved true error is small.
Excluded replay diagnostic	Saved failures with known true errors	Not used as decoder post-processing. A nontrivial logical operator extracted by comparing a syndrome-valid replay output with the saved true error is used only as a distance upper-bound witness or failure diagnostic, never as a FER-improving correction.

5 Finite-Length Frame Error Rate Measurements

This section reports the measured decoding performance for the constructed code. It defines the reference lines used in the FER figure, states how the plotted points should be interpreted, and separates these finite-sample measurements from any asymptotic threshold claim.

Figure 1 summarizes the decoding measurements for the constructed 64-fold lift. The horizontal axis is the depolarizing probability p , and the vertical axis is the FER. The hashing line is computed for the effective 64-fold-lift rate

$$R = 4108/10240 = 0.401171875$$

by solving the depolarizing-channel quantum hashing equation

$$1 - h_2(p) - p \log_2 3 = R.$$

The density-evolution (DE) line is an approximate binary-input BP density-evolution reference for the regular (3, 10) ensemble, not a finite-length threshold of this particular 64-fold-lift code. The use of hashing-bound and density-evolution reference lines is consistent with recent finite-length quantum LDPC decoding studies, but the present measurements are only for the single lifted code constructed here [8, 10, 30, 11]. The values used here are

$$p_{\text{hash}}(R = 4108/10240) = 0.09403285, \quad p_{\text{DE}}^{(3,10)} \approx 0.0733.$$

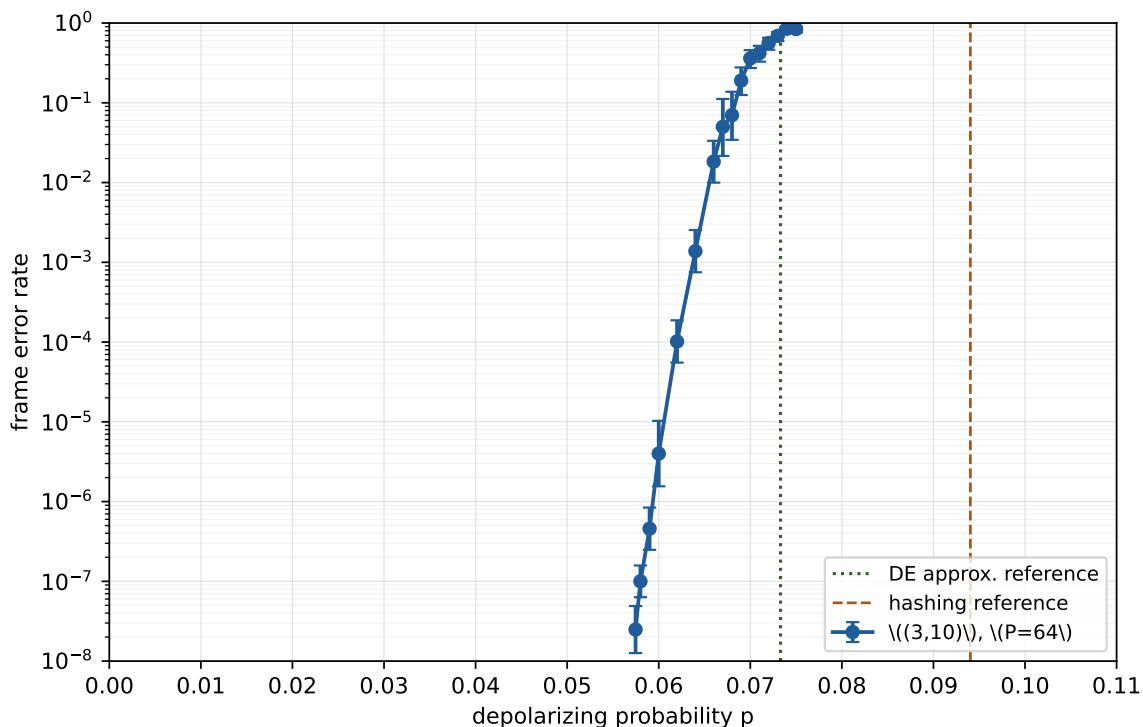


Figure 1: FER of the 64-fold lift for the $[[n, k, d]] = [[10240, 4108, 10 \leq d \leq 32]]$ CSS code. The hashing line is the depolarizing-channel quantum hashing bound for the effective rate $R = 4108/10240$. The DE line is an approximate BP density-evolution reference for the regular (3, 10) ensemble.

In the $p = 0.058$ run, joint BP with post-processing produced 25 recorded failures. The run contained 180,000,000 trials. The full post-processing rules correct 7 of these failures by the small-residual exact-search rule, leaving 18 failures after post-processing. The corrected FER is therefore

$$18/180,000,000 = 1.0 \times 10^{-7}.$$

This value uses only the deterministic post-processing rules in Table 2; it does not include any post-hoc logical-bank correction extracted from the recorded failures.

At the low- p side, the data include several measured points below and around $p = 0.060$, while higher- p points are used to show the transition range. These points should be read as finite-sample decoding measurements for the specific 64-fold lift and post-processing rules, not as an asymptotic threshold estimate. In the recorded decoding data, we did not observe a verified logical-error event or a smaller logical-error witness below the explicit weight-32 witnesses in Proposition 4. This

observation is not a proof of the exact minimum distance, because a distance lower bound requires exhaustive exclusion of all nontrivial logical representatives below the target weight. Nevertheless, within the present finite-length evidence, the absence of observed logical errors supports the interpretation that the actual minimum distance is likely closer to the certified upper-bound value 32 than to the conservative certified lower bound 10.

6 Discussion

The paper should be read first as a base-construction paper. The two-branch finite-field rule gives a structured way to build regular CSS LDPC bases, and the quotient-coset conditions make regularity, CSS orthogonality, and same-type 4-cycle exclusion checkable by finite computation. Table 1 records that this construction method is not limited to the detailed $(3, 10)$ case.

The $(3, 10)$ base is the finite-length case carried through the later stages of the paper. For that case, the base incidence pattern gives exact $(3, 10)$ regularity, CSS orthogonality, and the absence of same-type 4-cycles. The 64-fold cyclic lift prevents the remaining same-type base 6-cycles from closing, and the same lift labels are constrained to exclude the known weight-16 Z -type logical-support orbit.

These certificates do not prove the exact minimum distance. They show that the detailed finite-length example excludes the specified short-cycle condition and the specified weight-16 support pattern, while complete enumeration below weight 10 and certified logical witnesses give the finite bounds $10 \leq d \leq 32$. The decoding data then give a separate performance measurement for the verified lift under joint BP and deterministic post-processing. No logical error was observed in these decoding records, and no smaller logical witness than the certified weight-32 representatives was identified. Thus the experimental evidence is consistent with the minimum distance being close to the upper end of the certified interval, although the rigorous statement remains $10 \leq d \leq 32$. For the other (J, L) -regular bases in Table 1, the same two-branch construction already supplies the base matrices; choosing lifts, certifying distance-relevant structures, and measuring finite-length decoding performance for those parameter pairs are left for future work. One concrete plan is to strengthen the base stage itself. If one can construct regular CSS bases whose same-type Tanner graphs already have girth at least eight, then the lift stage no longer has to impose nonzero congruence constraints for base 6-cycle exclusion. The cyclic-lift search would then mainly enforce the zero congruence constraints required for CSS orthogonality, together with a smaller set of nonzero constraints for explicitly targeted low-weight support patterns. This would make the lift-label problem easier and would provide a cleaner route to larger finite-length examples. Another direction is to remove the finite-field restriction from the base construction. The proofs indicate that the essential object is a finite translation set with a free action on the relevant nonzero differences, not necessarily a field. Developing the corresponding orbit-based construction over finite groups, rings, or modules may produce further regular CSS bases beyond those accessible through multiplicative subgroups of finite fields.

References

- [1] R. G. Gallager, “Low-density parity-check codes,” *IRE Transactions on Information Theory*, vol. 8, no. 1, pp. 21–28, 1962.
- [2] T. J. Richardson and R. L. Urbanke, “The capacity of low-density parity-check codes under message-passing decoding,” *IEEE Transactions on Information Theory*, vol. 47, no. 2, pp. 599–618, 2001.

- [3] T. J. Richardson, M. A. Shokrollahi, and R. L. Urbanke, “Design of capacity-approaching irregular low-density parity-check codes,” *IEEE Transactions on Information Theory*, vol. 47, no. 2, pp. 619–637, 2001.
- [4] C. A. Kelley and J. L. Walker, “LDPC codes from voltage graphs,” in *2008 IEEE International Symposium on Information Theory*, 2008.
- [5] K. Okada and K. Kasai, “Random construction of quantum LDPC codes,” *arXiv preprint arXiv:2511.04634*, 2025.
- [6] A. R. Calderbank and P. W. Shor, “Good quantum error-correcting codes exist,” *Physical Review A*, vol. 54, no. 2, pp. 1098–1105, 1996.
- [7] A. M. Steane, “Multiple-particle interference and quantum error correction,” *Proceedings of the Royal Society of London. Series A: Mathematical, Physical and Engineering Sciences*, vol. 452, no. 1954, pp. 2551–2577, 1996.
- [8] D. Komoto and K. Kasai, “Quantum error correction near the coding theoretical bound,” *npj Quantum Information*, vol. 11, p. 154, 2025.
- [9] K. Kasai, “Efficient mitigation of error floors in quantum error correction using non-binary low-density parity-check codes,” *arXiv preprint arXiv:2501.13923*, 2025.
- [10] —, “Quantum error correction exploiting degeneracy to approach the hashing bound,” *arXiv preprint arXiv:2506.15636*, 2025.
- [11] —, “Breaking the orthogonality barrier in quantum LDPC codes,” *arXiv preprint arXiv:2601.08824*, 2026.
- [12] D. J. C. MacKay, G. Mitchison, and P. L. McFadden, “Sparse-graph codes for quantum error correction,” *IEEE Transactions on Information Theory*, vol. 50, no. 10, pp. 2315–2330, 2004.
- [13] D. Poulin and Y. Chung, “On the iterative decoding of sparse quantum codes,” *Quantum Information and Computation*, vol. 8, no. 10, pp. 987–1000, 2008.
- [14] M. Hagiwara and H. Imai, “Quantum quasi-cyclic LDPC codes,” in *2007 IEEE International Symposium on Information Theory*, 2007, pp. 806–810.
- [15] S. A. Aly, “A class of quantum LDPC codes constructed from finite geometries,” in *2008 IEEE Global Telecommunications Conference*, 2008, pp. 1097–1101.
- [16] D. Komoto and K. Kasai, “Explicit construction of quantum quasi-cyclic low-density parity-check codes with column weight 2 and girth 12,” *arXiv preprint arXiv:2501.13444*, 2025.
- [17] K. Kasai, “Quantum error correction with girth-16 non-binary LDPC codes via affine permutation construction,” *arXiv preprint arXiv:2504.17790*, 2025.
- [18] —, “Systematic non-binary extension of LDPC-CSS codes preserving orthogonality,” *arXiv preprint arXiv:2510.25583*, 2025.
- [19] J.-P. Tillich and G. Zemor, “Quantum LDPC codes with positive rate and minimum distance proportional to the square root of the blocklength,” *IEEE Transactions on Information Theory*, vol. 60, no. 2, pp. 1193–1202, 2014.
- [20] M. B. Hastings, J. Haah, and R. O’Donnell, “Fiber bundle codes: Breaking the $N^{1/2}$ polylog(N) barrier for quantum LDPC codes,” in *Proceedings of the 53rd Annual ACM SIGACT Symposium on Theory of Computing*, 2021, pp. 1276–1288.

- [21] P. Panteleev and G. Kalachev, “Asymptotically good quantum and locally testable classical LDPC codes,” in *Proceedings of the 54th Annual ACM SIGACT Symposium on Theory of Computing*, 2022, pp. 375–388.
- [22] A. Leverrier and G. Zemor, “Quantum tanner codes,” in *Proceedings of the 63rd IEEE Annual Symposium on Foundations of Computer Science*, 2022, pp. 872–883.
- [23] K. Kasai, “Finite-degree quantum LDPC codes reaching the gilbert–varshamov bound,” *arXiv preprint arXiv:2603.24588*, 2026.
- [24] P. Panteleev and G. Kalachev, “Degenerate quantum LDPC codes with good finite length performance,” *Quantum*, vol. 5, p. 585, 2021.
- [25] N. P. Breuckmann and J. N. Eberhardt, “Quantum low-density parity-check codes,” *PRX Quantum*, vol. 2, p. 040101, 2021.
- [26] K. Kasai, “Heuristic search for minimum-distance upper-bound witnesses in quantum APM-LDPC codes,” *arXiv preprint arXiv:2604.15307*, 2026.
- [27] K. Okada and K. Kasai, “High-girth regular quantum LDPC codes from affine-coset structures,” *arXiv preprint arXiv:2604.20838*, 2026.
- [28] —, “High-girth regular quantum LDPC codes from square-base hypergraph products via CPM lifts,” *arXiv preprint arXiv:2604.27817*, 2026.
- [29] K. Kasai, “A factor-graph formulation of CSS syndrome decoding: Joint BP and four-state BP,” *arXiv preprint arXiv:2605.05132*, 2026. [Online]. Available: <https://arxiv.org/abs/2605.05132>
- [30] D. Komoto and K. Kasai, “Sharp error-rate transitions in quantum QC-LDPC codes under joint BP decoding,” in *2025 IEEE International Conference on Quantum Computing and Engineering (QCE)*, vol. 2, 2025, pp. 564–565.